

<sup>9</sup>L. Tonks and I. Langmuir, *Phys. Rev.* **34**, 876 (1929). Equation (2) is for the case when the ionization rate is proportional to the plasma electron density.

<sup>10</sup>D. A. Dunn and S. A. Self, *J. Appl. Phys.* **35**, 113 (1964).

<sup>11</sup>W. Lotz, *Astrophys. J., Suppl. Ser.* **14**, 207 (1967).

## Sound Absorption and Dispersion along the Critical Isochore in Xenon\*

Don Eden,<sup>†</sup> Carl W. Garland, and Jan Thoen<sup>‡</sup>

*Department of Chemistry and Center for Materials Science and Engineering,  
Massachusetts Institute of Technology, Cambridge, Massachusetts 02139*

(Received 17 January 1972)

Ultrasonic and Brillouin absorption and velocity data along the critical isochore in xenon are reinterpreted in terms of modified theoretical expressions derived within the framework of the Fixman-Mistura theory. The new expressions mainly arise from avoiding the unjustified assumption of small dispersion near a liquid-gas critical point. Numerical analysis of the data shows quite satisfactory agreement between theory and experiment for both sound absorption and dispersion.

In this Letter we report a modification to the theory of critical sound propagation in pure simple fluids and present a reanalysis of some recent experimental data for absorption and dispersion along the critical isochore in xenon. Mode-mode coupling theory has been developed in considerable detail by Kawasaki<sup>1</sup> to describe acoustic absorption and dispersion near a liquid-gas critical point. Recently, Mistura<sup>2</sup> developed a modified version of Fixman's original approach<sup>3</sup> involving energy transfer between sound waves and density fluctuations and obtained results identical to those presented by Kawasaki. In both the Kawasaki and Mistura derivations, the velocity dispersion is assumed to be small. Although this is a good assumption for the closely related problem of critical phase separation in binary fluids, it is a poor approximation for pure fluids. The new expressions for absorption and dispersion presented below have been obtained without making this assumption.

In a previous Letter<sup>4</sup> new experimental results for sound absorption in xenon were reported in the frequency range between 0.4 and 5 MHz and interpreted in terms of the previously cited theories.<sup>1,2</sup> Hypersonic attenuation values from Brillouin linewidths<sup>5</sup> were also discussed. The essential result was that the critical sound absorption per wavelength (defined as the difference between the observed absorption and the classical absorption) depended only on a single reduced variable  $\omega^* = \omega/\omega_D$ , with the characteristic frequency for thermal diffusion defined by

$$\omega_D = (2\Lambda/\rho C_p)\xi^{-2}, \quad (1)$$

where  $\Lambda$  is the thermal conductivity coefficient,

$C_p$  is the specific heat at constant pressure,  $\rho$  is the density, and  $\xi$  is the correlation length.

Good agreement between theory and experiment could, however, only be obtained for  $\omega^* \lesssim 2$ . For higher  $\omega^*$ , the experimental  $\alpha_\lambda$  values increased monotonically and then leveled off at a constant value independent of  $\omega^*$ , whereas the theory predicted a decrease in  $\alpha_\lambda$  with increasing  $\omega^*$  values above  $\omega^* \approx 8$ . The behavior of  $\alpha_\lambda$  as a function of  $\omega^*$  in xenon was also in contrast with the experimental results for binary liquid systems where a decrease in  $\alpha_\lambda$  has been observed at large  $\omega^*$  values.<sup>2,6</sup>

In a simultaneously published Letter by Cummins and Swinney<sup>7</sup> an analysis of sound-dispersion data obtained from Brillouin and ultrasonic work was made in terms of the theoretical predictions of Kawasaki.<sup>1</sup> It was found that the dispersion in the Brillouin data and in the ultrasonic data could be separately described reasonably well with different sets of adjustable parameters, but the dispersion in the Brillouin velocities seem to be 2 to 3 times smaller than the theory predicted when values of the parameters obtained from the ultrasonic experiment were used.

The reanalysis of these experimental data in terms of our new expressions for  $\alpha_\lambda$  and for the dispersion will show that the large discrepancies cited above and discussed in Refs. 2, 4, and 7 are artifacts which disappear when the correct theoretical expressions are used.

We will follow the Fixman-Mistura approach and introduce a complex sound velocity  $u^*$  which is related to a complex frequency-dependent excess specific heat  $\Delta$  by

$$u^{*2} = u_T^2(C_p + \Delta)/(C_v + \Delta), \quad (2)$$

where  $u_T$  is the isothermal sound velocity. From the exact expressions for the velocity,  $1/u(\omega) = \text{Re}(1/u^*)$ , and the amplitude absorption coefficient,  $\alpha(\omega) = \omega \text{Im}(1/u^*)$ , and from the definition  $u^* = u' + iu''$ , one can easily show that

$$u^2(\omega) = \text{Re}(u^{*2}) = u'^2, \quad (3)$$

$$\alpha_\lambda(\omega) = -\pi u^{-2}(\omega) \text{Im}(u^{*2}) = -2\pi u''/u'$$

if  $(u''/u')^2 = (\alpha_\lambda/2\pi)^2 \ll 1$ . This condition is well satisfied for xenon since the  $\alpha_\lambda$  values analyzed below are always less than 0.5.

We shall now obtain explicit expressions for  $u(\omega)$  and  $\alpha_\lambda(\omega)$  in terms of the real and imaginary parts of  $\Delta$ . Using the quantity  $\tilde{C}_v \equiv C_v + \Delta$ , we can rewrite Eq. (2) as

$$u^{*2} = u^2(0) \left( 1 - \frac{C_p - C_v}{C_p \tilde{C}_v} \Delta \right), \quad (4)$$

where  $u(0)$  is the static adiabatic sound velocity. Now introducing the variable  $\Delta_1 \equiv \Delta/(1 + \Delta C_v^{-1}) \equiv \Delta_1' + i\Delta_1''$ , we can rewrite Eqs. (3) as

$$u^2(\omega) = u^2(0) [1 - (\gamma - 1) C_p^{-1} \Delta_1'], \quad (5)$$

$$\alpha_\lambda(\omega) = \pi u^2(0) u^{-2}(\omega) (\gamma - 1) C_p^{-1} \Delta_1'',$$

where  $\gamma = C_p/C_v$  is the ratio of static specific heats. If one assumed that the dispersion were small and that  $\Delta/C_v \ll 1$  everywhere, Eqs. (5) would immediately reduce to the expressions already obtained by Mistura.<sup>2</sup> Being more careful, we find

$$\frac{u^2(\omega) - u^2(0)}{u^2(\omega)} = -\frac{\gamma - 1}{C_p} \Delta', \quad (6)$$

$$\alpha_\lambda(\omega) = \frac{\pi u^2(\omega)}{u^2(0)} \frac{\gamma - 1}{C_p} \Delta''. \quad (7)$$

In deriving Eqs. (6) and (7), we have made use of the valid conditions  $(\Delta''/C_v)^2 \lesssim (\alpha_\lambda/\pi)^2 \ll 1$  and  $\Delta''^2/\Delta'(C_v + \Delta') \ll 1$  and the approximation  $1 + \Delta' C_v^{-1} \approx u^2(0)/u^2(\omega)$ . At this point, we can insert the previously determined<sup>2,4</sup> expressions for  $\Delta'$  and  $\Delta''$  to obtain

$$\alpha_\lambda(\text{crit}) = 2\pi u^2(\omega) A(\epsilon) I(\omega^*), \quad (8)$$

$$1 - u^2(0) u^{-2}(\omega) = 2u^2(0) A(\epsilon) J(\omega^*) \\ \equiv B(\epsilon) J(\omega^*), \quad (9)$$

$$A(\epsilon) = \frac{k_B T^3}{2\pi^2 \rho^3} \left( 1 - \frac{1}{2} \eta \right)^2 \frac{1}{u^4(0) C_v^2} \\ \times \left( \frac{\partial P}{\partial T} \right)^2 \kappa \left( \frac{\partial \kappa}{\partial T} \right)^2, \quad (10)$$

where  $\epsilon \equiv (T - T_c)/T_c$ ,  $\eta$  is the critical exponent

arising from the Fisher correction to the correlation function, and  $\kappa \equiv \xi^{-1}$  is the inverse correlation length.  $I(\omega^*)$  and  $J(\omega^*)$  represent the following integrals:

$$I(\omega^*) = \int_0^\infty \frac{x^2 dx}{(1+x^2)^2} \frac{\omega^* K(x)}{K^2(x) + \omega^{*2}}, \quad (11)$$

$$J(\omega^*) = \int_0^\infty \frac{x^2 dx}{(1+x^2)^2} \frac{\omega^{*2}}{K^2(x) + \omega^{*2}}, \quad (12)$$

where  $x = q\xi$  and  $K(x) = \frac{3}{4} [1 + x^2 + (x^3 - x^{-1}) \arctan x]$ .

In deriving Eq. (6) we assumed that  $\Delta''^2/\Delta' \times (C_v + \Delta') \ll 1$ . This is approximately equivalent to

$$\frac{1}{C_v} \frac{\kappa_B T^2}{\pi^2 \rho} \kappa \left( \frac{\partial \kappa}{\partial T} \right)^2 \frac{I^2(\omega^*)}{J(\omega^*)} \ll 1.$$

A numerical calculation of this quantity along  $\rho = \rho_c$  indicated that for the range of the present experimental data in xenon it did not become larger than 0.05.

We now want to report on the new analysis of the experimental results in xenon. The ultrasonic data are the same as those reported in Ref. 4 for the sound absorption and in Ref. 7 for the dispersion. The Brillouin data analyzed in these two references are also incorporated in the new analysis.

From our modified expression (8) it can be seen that  $\alpha_\lambda(\omega)/u^2(\omega)A(\epsilon)$  should depend only on the reduced frequency  $\omega^*$ . Consequently, we have combined the velocity and absorption data to obtain the new quantity  $\alpha_\lambda(\omega)u^{-2}(\omega)$  for further analysis. This could be done very well since the velocity and absorption readings were taken simultaneously. The experimental  $\alpha_\lambda(\omega)u^{-2}(\omega)$  data were then used in a least-squares fit of Eq. (8) to determine the adjustable parameters  $A_0$ ,  $z$ , and  $D$  in the expression  $A(\epsilon) = A_0 \epsilon^z (1 + D\epsilon)$  for the prefactor of  $I(\omega^*)$ . For the quantity  $\omega_D$  defined in Eq. (1), we used the same result,  $\omega_D = 5.38 \times 10^{12} \epsilon^2 \text{ sec}^{-1}$ , as in Ref. 4. This result was essentially based on the available experimental data for the total thermal diffusivity<sup>8</sup> and the correlation lengths.<sup>9</sup> For all the ultrasonic data, the critical temperature was taken to be 16.953°C, which was the observed temperature of the velocity minimum. With  $T_c$  as a free parameter in the least-squares fit, we obtained a value which differed from this by only a few hundredths of a degree and which did not substantially improve the quality of the fit to the data. The same choice of  $T_c$  was made in Ref. 4 and will be discussed in detail elsewhere.<sup>10</sup> The initial numeri-

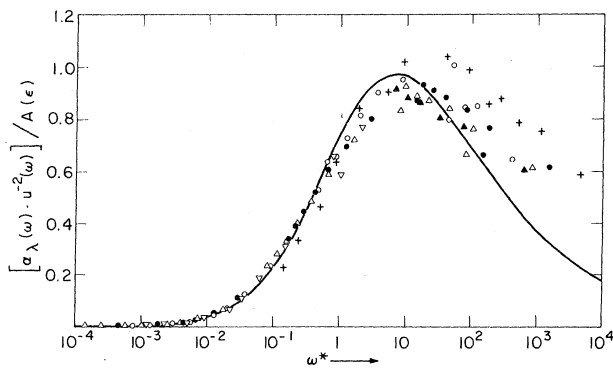


FIG. 1. Reduced critical sound attenuation per wavelength in Xe along the critical isochore above  $T_c$  as a function of the reduced frequency  $\omega^* = \omega/\omega_D$ . Ultrasonic data are shown at 0.4 (solid triangle), 0.55 (open triangle), 1 (solid dot), 3 (open dot), and 5 MHz (inverted triangle). Hypersonic values at  $\sim 500$  MHz (pluses) were obtained from Brillouin linewidths. The solid curve represents  $2\pi I(\omega^*)$ , where the integral  $I(\omega^*)$  is defined in Eq. (11).

cal analysis indicated that the effect of the parameter  $D$  was very small; thus  $D$  was zero in all further analysis. In Fig. 1 we have plotted  $\alpha_\lambda(\omega) \times u^{-2}(\omega)/A(\epsilon)$  versus  $\omega^*$  with  $A_0 = 7.3 \times 10^{-6} m^{-2} \text{ sec}^2$ ,  $z = -0.22$ , and  $D = 0$ . According to Eq. (8) all the experimental points should fall on a single curve represented by  $2\pi I(\omega^*)$ . Within the experimental scatter, which is rather large near  $T_c$  because of the combined errors in the two quantities  $\alpha_\lambda(\omega)$  and  $u^2(\omega)$ , this requirement seems to be largely fulfilled by the ultrasonic data. There remain, however, two small discrepancies: The maximum in the experimental data seems to occur at a larger  $\omega^*$  value than that predicted by  $I(\omega^*)$ , and the experimental data lie systematically above the theoretical curve for large  $\omega^*$  values. Both of these effects can probably be ascribed to the breakdown for large  $\omega^*$  of the assumption of an Ornstein-Zernike form for the behavior of the fluctuations, which was introduced in the derivation of the expression for  $\Delta$ .<sup>2,4</sup> These discrepancies are even more pronounced for the results derived from the Brillouin data of Cannell.<sup>5</sup> It should, however, be noted that there are even larger uncertainties associated with the hypersonic points in Fig. 1, since a rather large, not too well-known background classical absorption had to be subtracted.<sup>4</sup> In spite of these small discrepancies between theory and experiment, we believe that Fig. 1 shows that if one plots the correct quantity, in this case  $\alpha_\lambda(\omega)u^{-2}(\omega)A^{-1}(\epsilon)$ , the large qualitative difference thought to exist between the behavior

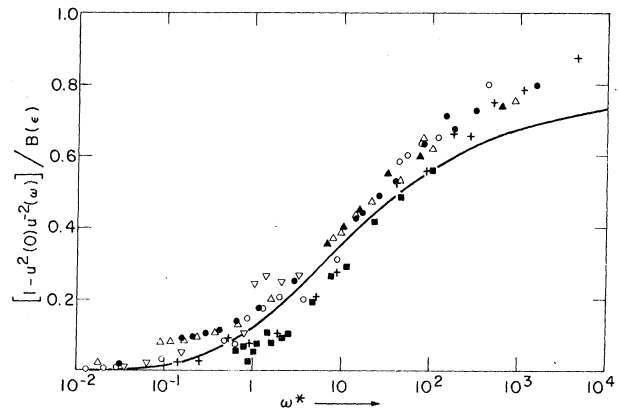


FIG. 2. Reduced sound dispersion in Xe along the critical isochore above  $T_c$  as a function of the reduced frequency  $\omega^* = \omega/\omega_D$ . Ultrasonic data are shown at 0.4 (solid triangle), 0.55 (open triangle), 1 (solid dot), 3 (open dot), and 5 MHz (inverted triangle). Hypersonic values at  $\sim 500$  MHz (pluses) and  $\sim 170$  MHz (solid squares) were obtained from Brillouin data. The solid curve represents the integral  $J(\omega^*)$  defined in Eq. (12).

of binary mixtures and simple fluids disappears. Moreover, the least-squares value of  $z$  is completely consistent with the most recent value of the critical exponent  $\nu$ . Our value of  $z = 3\nu - 2$  leads to  $\nu = 0.59$ , in good agreement with the value  $0.58 \pm 0.05$  reported by Smith, Giglio, and Benedek.<sup>11</sup>

In principle, one can carry out a similar least-squares fit for the quantity  $1 - u^2(0)u^{-2}(\omega)$ . It should, however, be emphasized that for much of the data this quantity does not differ greatly from zero, and relatively large absolute errors have to be considered in fitting these results. Instead of fitting these data by least squares directly, we have followed what we believe to be a more reliable procedure. Values of the prefactor  $B(\epsilon)$  in Eq. (9) have been calculated using  $A(\epsilon)$  values from the least-squares fit of the absorption and  $u(0)$  data.<sup>12</sup> The  $u(0)$  data used in the calculations were based on our 0.55-MHz results far from the critical point and on low-frequency ( $\sim 10$  kHz) results of Carome<sup>13</sup> and on values calculated from the  $C_v$  results of Edwards, Lipa, and Buckingham<sup>14</sup> for the temperature range close to  $T_c$ . In Fig. 2 experimental values of the quantity  $[1 - u^2(0)u^{-2}(\omega)]/B(\epsilon)$  are compared as a function of  $\omega^*$  with the theoretical predicted values given by the integral  $J(\omega^*)$ . We obtain again rather good agreement between theory and experiment. Two discrepancies should, however, be noted. For the  $\omega^*$  range between 1 and 10, the

Brillouin results seem to be systematically lower than the ultrasonic data and lower than the theoretical integral  $J(\omega^*)$ .<sup>15</sup> We also find that the theoretically predicted dispersion is too small at large  $\omega^*$  values. Probably the same argument about the assumption of the Ornstein-Zernike form should be invoked here. It should, however, be emphasized that the previously reported<sup>7</sup> large discrepancies between the Brillouin and ultrasonic dispersion results have disappeared and that a reasonably good agreement with theory can now be obtained.

\*Research supported in part by the Advanced Research Projects Agency, and in part by the National Science Foundation.

†Presently at the Department of Physics, New York University, New York, N. Y. 10003.

‡On leave from the Division of Molecular Physics, Department of Physics, University of Leuven, Leuven, Belgium; supported in part by NATO.

<sup>1</sup>K. Kawasaki, *Phys. Rev. A* **1**, 1750 (1970).

<sup>2</sup>L. Mistura, in "International School of Physics 'Enrico Fermi,' Course LI," edited by M. S. Green (Academic, New York, to be published).

<sup>3</sup>M. Fixman, *J. Chem. Phys.* **33**, 1363 (1960), and **36**, 1961 (1962).

<sup>4</sup>C. W. Garland, D. Eden, and L. Mistura, *Phys. Rev. Lett.* **25**, 1161 (1970); see also D. Eden, Ph.D thesis, Massachusetts Institute of Technology, 1971 (unpub-

lished).

<sup>5</sup>D. S. Cannell and G. B. Benedek, *Phys. Rev. Lett.* **25**, 1157 (1970); D. S. Cannell, Ph.D. thesis, Massachusetts Institute of Technology, 1970 (unpublished).

<sup>6</sup>G. D'Arrigo, L. Mistura, and P. Tartaglia, *Phys. Rev. A* **3**, 1718 (1971).

<sup>7</sup>H. Z. Cummins and H. L. Swinney, *Phys. Rev. Lett.* **25**, 1165 (1970).

<sup>8</sup>D. L. Henry, H. L. Swinney, and H. Z. Cummins, *Phys. Rev. Lett.* **25**, 1170 (1970).

<sup>9</sup>M. Giglio and G. B. Benedek, *Phys. Rev. Lett.* **23**, 1145 (1969).

<sup>10</sup>P. E. Mueller, D. Eden, C. W. Garland, and R. C. Williamson, to be published.

<sup>11</sup>I. W. Smith, M. Giglio, and G. B. Benedek, *Phys. Rev. Lett.* **27**, 1556 (1971).

<sup>12</sup>It should be noted here that for the investigated temperature range  $B(\epsilon)$  turned out to be almost constant. The theoretical expression for  $\pi B(\epsilon)$  is the same as that for the  $B$  in Eq. (6) of Ref. 4. The value of  $\pi B(\epsilon)$  varied in our new analysis between 2.0 and 1.8. This should be compared with the constant value of 1.9 which was adopted for  $B$  in Ref. 4.

<sup>13</sup>E. F. Carome, private communication.

<sup>14</sup>C. Edwards, J. A. Lipa, and M. J. Buckingham, *Phys. Rev. Lett.* **20**, 496 (1968).

<sup>15</sup>It has been pointed out to us by H. L. Swinney that in the derivation of the integrals given in Eqs. (11) and (12), only the critical part of the Rayleigh linewidth is introduced. The maximum difference in the value for the integrals between the assumption that the total linewidth equals the critical linewidth or equals only the background value is however not more than 20% at  $\omega^* \approx 5$ . The effect is much smaller for  $I(\omega^*)$  than for  $J(\omega^*)$ .

## Solid Phase of He<sup>4</sup> Monolayers: Debye Temperatures and "Melting" Anomalies\*

M. Bretz, G. B. Huff, and J. G. Dash

*Department of Physics, University of Washington, Seattle, Washington 98105*

(Received 7 February 1972)

Specific heats of He<sup>4</sup> monolayers on graphite indicate two-dimensional solid phases. Debye temperatures  $\Theta$  range from 17.6° to 56° systematically with coverage. Anomalies are identified with melting, but the melting process is a continuous transition. Films and bulk solid He<sup>4</sup> at equal values of interatomic spacing have nearly the same  $\Theta$ 's and melting temperatures.

Low-coverage He monolayers on basal-plane graphite surfaces behave as two-dimensional (2D) quantum gases.<sup>1,2</sup> At higher densities, He<sup>3</sup> and He<sup>4</sup> display sharp second-order heat-capacity peaks attributed to lattice-gas-ordering transitions.<sup>3</sup> In this Letter we describe new features at still higher coverages: a 2D solid regime closely analogous to bulk solid He<sup>4</sup> which melts by a continuous process.

This study was made with the same apparatus and procedures as before. The films were twelve samples of He<sup>4</sup>, at coverages  $x$  between 0.7 and 1.16. We define  $x \equiv N/N_m$ , where  $N_m = 96 \text{ cm}^3 \text{ STP}$  is the He<sup>4</sup> monolayer capacity of the graphite calorimeter at low  $T$ . Film specific heats  $C/Nk$  are given in Fig. 1, much of the data being omitted for greater clarity. We include data near 3° for He<sup>4</sup> at the "critical coverage"  $x_c$  of the ordering